J. Coat. Technol. Res.
https://doi.org/10.1007/s11998-023-00839-7

POSS-vinyl-urethane acrylate-based nanohybrid coating materials

Yasemin Eren, Ferhat Şen, Suzan Abdurrahmanoğlu, Sevim Karataş

Received: 6 December 2022 / Revised: 17 July 2023 / Accepted: 18 July 2023

Abstract The effect of POSS-vinyl-heptaisobutyl-substituted (POSSV) compounds as an inorganic additive on the thermal and physical properties of nanohybrid coating materials based on urethane acrylate (UA) resin has been investigated. A diol compound obtained from the reaction of itaconic acid and 1,2-epoxy cyclohexane has been used to produce an UV curable epoxy-based urathane acrylate resin. Nanohybrid coating materials were obtained by curing the UA resin with UV radiation through the thiol–ene reaction, mixed with various amounts of POSSV compounds. The structure of the UA resin was characterized by Fourier-transform infrared spectroscopy and nuclear magnetic resonance spectroscopy techniques. The UV curing process was also studied by the double bond conversion method. Aggregation of the nanohybrid materials was determined by X-ray diffraction. The thermal, non-flammability, and thermomechanical properties of the samples were examined by thermogravimetric analysis, limiting oxygen index, and dynamic mechanical analysis techniques. Light transmittance of the samples was determined by UV–Vis spectrophotometry, and their morphological structure was determined by scanning electron microscopy. In addition, gel contents, swelling rates, hardness, adhesion, contact angles, and resistance to chemicals and solvents of the samples were examined. In conclusion, nanohybrid materials obtained from the synthesized UA resin and improved with POSSV additive can be used in the coating industry.

Keywords UV-cured, Thiol–ene click, Urethane acrylate

Supplementary Information The online version contains supplementary material available at https://doi.org/10.1007/s11998-023-00839-7.

Y. Eren, S. Abdurrahmanoğlu, S. Karataş (✉)
Department of Chemistry, Marmara University, 34722 Istanbul, Turkey
e-mail: skaratas@marmara.edu.tr

F. Şen
Department of Nanotechnology Engineering, Zonguldak Bülent Ecevit University, 67100 Zonguldak, Turkey

Introduction

The importance of organic–inorganic hybrid coating materials has increased in recent years due to the possession of both advantageous organic and inorganic properties, which allows the forming of a well-structured material on a molecular level.[1–3] Various types of inorganic additives such as fullerene, silicon dioxide, POSS (polyhedral oligomeric silsesquioxane), graphene, and carbon nanotubes have been used to prepare these hybrid coating materials with polymers as inorganic parts.[4,5] The synthesis conditions can be designed to obtain a coating material which possesses the desired properties.

Polyurethane (PU)-based polymers with their excellent mechanical properties have been mostly used for the preparation of coating materials, adhesives, elastomers, etc.[6] Conventional PU forms in the reaction of polyol resins and polyisocyanate, and the properties of the final product strongly depend on the synthesis process besides the type of these two precursors.[7, 8] Traditional PUs contain significant amounts of organic solvents and a free isocyanate monomer moiety. Due to the recent regulations for environmental protection, bio-based materials such as herbal oils, acids, and dicarboxylic acids have been used in the synthesis of coating materials rather than petroleum derivatives.[9] Itaconic acid, an unsaturated dicarbonic acid, is a renewable material which can be produced by a fungi (*Aspergillus terreus*) from sugar.[10] It has been used for

Published online: 08 November 2023

the synthesis of various resins, such as polyester, epoxy, etc.[11,12]

UV-curing technology is one of the most environmentally friendly methods, due to the numerous advantages, such as short reaction time, lower energy consumption, etc., used in various industrial areas.[13,14] This technology has been considered an alternative to the conventional solvent-based methods due to the environmental issues.[15] This process usually progresses through the compounds which possess unsaturated bonds such as urethane acrylates by free radical formation.[16] In this case, the rigid hard segment consists of polyester polyols and the flexible soft segment consists of isocyanate and acrylate, such as hydroxyethyl methacrylate (HEMA).[17] Polyurethane acrylates are generally used as oligomers to improve the physical and mechanical properties, such as adhesion and heat and chemical resistance for UV-curable coating systems.[18] On the other hand, the nanosized inorganic particles have recently also been attractive materials to obtain polymer coatings with excellent mechanical properties.[19] The nanoscale interaction between organic and inorganic components provides a more efficient and economical method for the synthesis of well-designed coating materials.[20,21]

Nanohybrid materials can be synthesized by various mechanisms but commonly by using inorganic materials such as POSS which are considered as nanobuilding blocks with their well-defined structures.[22] In this method, the properties of final coating materials can be predictable since the molecular units keep their structures throughout the matrix formation. Moreover, the addition of POSS compounds to polymers provides a significant improvement in the properties of hybrid materials, such as thermal and mechanical stability, flammability resistance, electrical insulation, etc.[23]

In this work, we aimed to examine the effect of PSS-vinyl-heptaisobutyl-substituted (POSSV) compounds as an inorganic additive on the thermal and physical properties of nanohybrid coating materials based on urethane acrylate (UA) resin. Initially, a diol compound was synthesized starting from itaconic acid and 1,2-epoxy cyclohexane. This diol compound was reacted with isophorone diisocyanate (IPDI) and 2-HEMA to obtain UA as a UV-curable oligomer. Synthesized UA resin was mixed with various amounts of POSSV compound and cured by UV radiation through the thiol–ene reaction. The obtained nanohybrid UA resin was finally subjected to several analyses to characterize it by means of its thermal, microstructural, mechanical, and morphological properties.

Experimental

Materials

POSSV, 2-hydroxy-2-methylpropiophenon (Darocur 1173), triphenylphosphin (TPP), pentaerythritol tetraacrylate (PETA), pentaerythritol tetrakis(3-mercaptopropionate) (PETMP), *N*-vinyl pyrrolidone (NVP) and acetone were purchased from Sigma Aldrich. 1,2-epoxy cyclohexane and itaconic acid were purchased from Tokyo Chemical and used without further purification. IPDI was obtained from Alfa Aeser, HEMA, hydroquinone, tetrahydrofuran (THF), hydrochloric acid (HCl), acetic acid (CH_3COOH), sulfuric acid (H_2SO_4), sodium hydroxide (NaOH), chloroform, xylene, and methanol from Merck, and dibutyltin dilaurate (DBTDL) from Henkel.

Synthesis of epoxy-based urethane acrylate resin

The UA resin was synthesized according to the following procedure. Briefly, 1,2-epoxy cyclohexane (25.026 g), itaconic acid (16.575 g), and TPP (0.208 g) were loaded into a three-necked flask and heated to 100°C by using an oil bath. The reaction mixture was stirred for 1 h and then the temperature was set to 110°C. After 5 h stirring under nitrogen atmosphere, 41.809 g diol compounds were obtained.

IPDI (56.371 g) and DBTDL (0.13 g) were gradually added to the diol compounds drop by drop through a funnel for 2 h. The progress of the reaction was kept under control by Fourier-transform infrared (FTIR) measurements. After 2 h, hydroquinone (0.1572 g) was added under continous stirring. –NCO-terminated urethane resin was obtained from this reaction.

HEMA (33.212 g) was gradually loaded onto the –NCO-terminated urethane resin for 1 h at 40°C. Then, the reaction was carried out for 3 h under a nitrogen atmosphere at 50°C and then stopped when the –NCO bands disappeared in the FTIR spectrum. The final product was dried in a vacuum oven at 45°C to remove the acetone. The structure of the epoxy-based urethane resin was identified by FTIR and ^{1}H-NMR analyses. The synthesis of the UA resin is shown in Fig. 1.

Preparation of UV curable nanohybrid coating materials

UV-curable formulations were prepared by adding certain amounts of synthesized UA resin, NVP, PETA, PETMP, and Darocur 1173 as the photoinitator. In addition, POSSV dissolved in THF was added to the formulations at different ratios (1%, 3%, 5%, and 7% of the total formulation). All the formulations given in Table 1 were mixed by using an ultrasonic bath to avoid air bubbles and to obtain an homogeneous solution at 50°C. All the homogeneous UA nanohybrid formulations were subjected to a polymerization reaction on Teflon plates (50 mm x 10 mm × 1 mm) under a UV lamp (Osram Ultrawitt 300) for 3 min. Images of the obtained UA resin and nanohybrid materials are shown in Fig. 2.

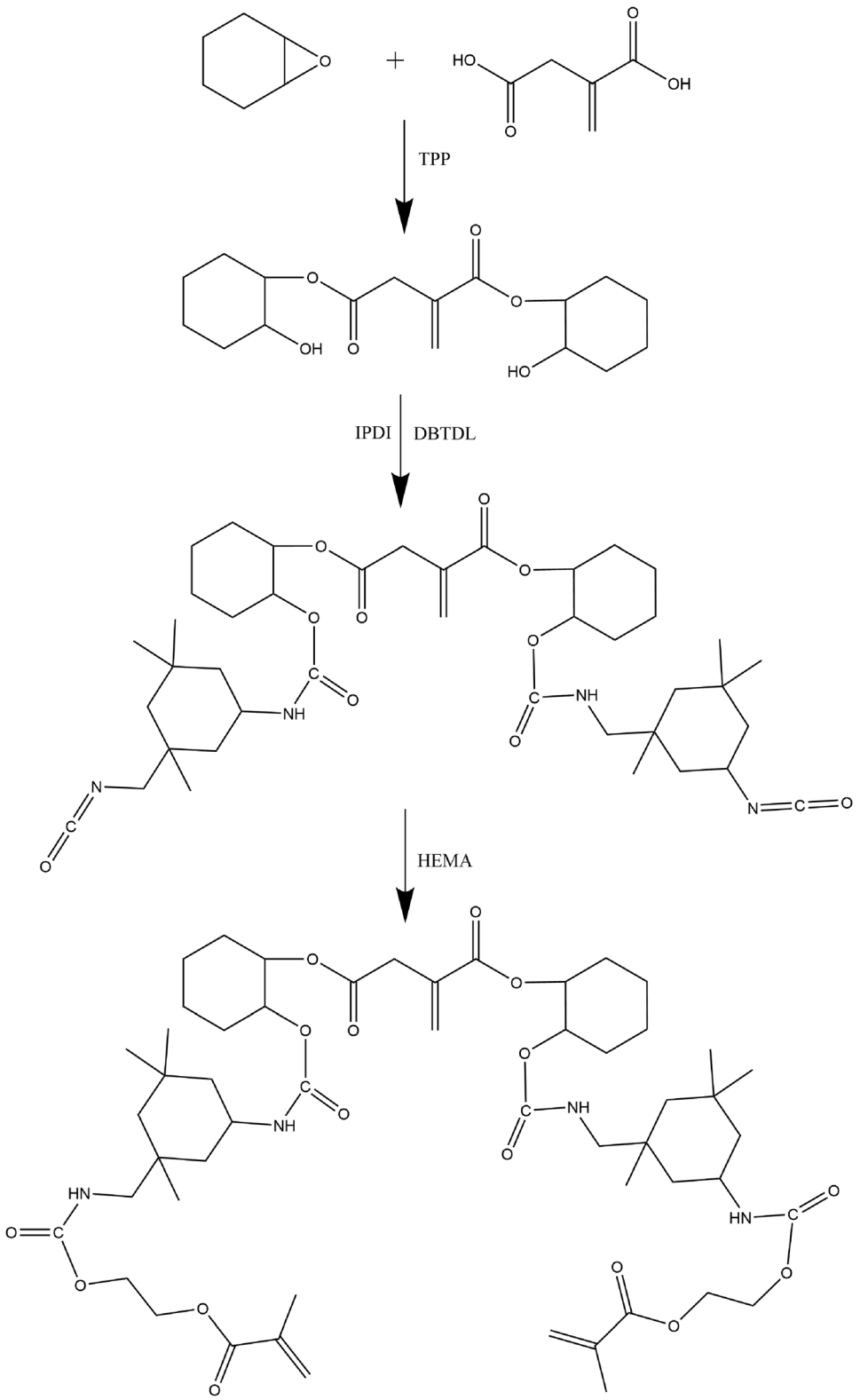

Fig. 1: Synthesis of epoxy-based urethane acrylate resin

Table 1: Formulations of nanohybrid coatings materials

Sample	UA (wt%)	NVP (wt%)	PETA (wt%)	PETMP (wt%)	Darocur 1173 (wt%)	POSSV (wt%)
UA	52	15	10	20	3	–
UA-POSSV:1	52	15	10	20	3	1
UA-POSSV:3	52	15	10	20	3	3
UA-POSSV:5	52	15	10	20	3	5
UA-POSSV:7	52	15	10	20	3	7

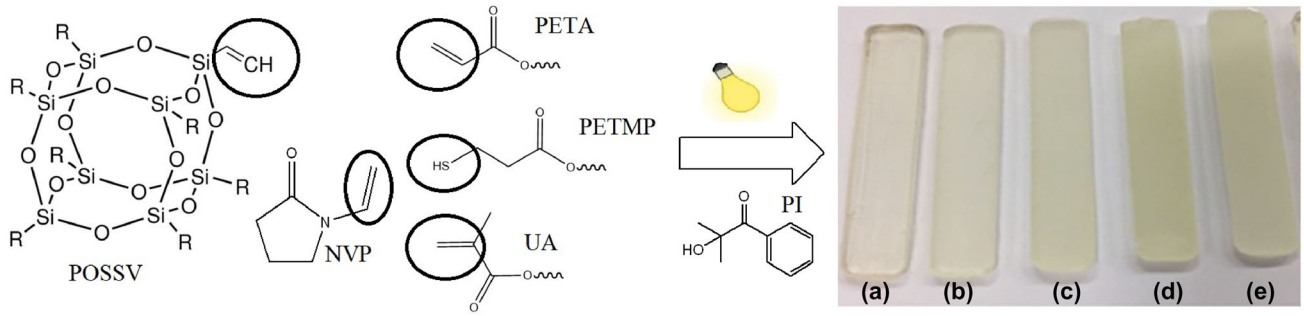

Fig. 2: Images of UA resin and nanohybrid materials: (a) UA, (b) UA-POSSV:1, (c) UA-POSSV:3, (d) UA-POSSV:5, (e) UA-POSSV:7

Characterization

The chemical structures of the UA resin and coating materials were examined by a Perkin Elmer ATR FTIR spectrophotometer,

^{1}H NMR spectra were performed on a Varian Mercury-VX400 BB model NMR, and ^{1}H NMR was accomplished using deuterated acetone (CD_3COCD_3) as the solvent.

The aggregation of the coating materials was determined by using an X-ray diffractometer (XRD; PANalytical X'Pert PRO) at a generator voltage of 45 kV and a current of 40 mA. The scattering angle was in the range of $2\theta = 2° - 40°$.

Thermo-oxidative stabilities of the coating materials were determined by heating them from 30°C to 800°C at a 10°C/min heating rate under air using a Perkin Elmer thermogravimetric analyzer.

The loss on ignition (LOI) was determined to characterize the fire-retardant performances of the samples. The coating materials were fixed into a glass cylinder and a slow stream of oxygen/nitrogen gas mixture was passed through the system. The minimum oxygen concentration required to support the ignition of the samples for 180 s were determined.

Dynamic mechanical analysis (DMA) was carried out on a Perkin Elmer-DMA 8000 using the Centilever mode. The dynamic storage modulus was determined at a frequency of 1 Hz. The temperature range was set from 30°C to 100°C at a heating rate of 3°C/min.

UV–Vis spectra of the coating materials were recorded using a Shimadzu UV-2450 spectrophotometer to examine their permeability.

The Soxhlet extraction method was used to determine the gel content of the samples. Briefly, the weighed film samples were extracted with acetone for 4 h and dried in a vacuum oven at 50°C, then weighed again and the gel contents were calculated.

Absorption tests were applied to all the prepared nanohybrid film samples in order to determine their water resistance. Dry film samples were weighed and immersed into distilled water for 24 h, then the wet film samples were weighed and their equilibrium swelling ratios were calculated.

A Gardco Paint Adhesion Kit was used to test the adhesion properties of the nanohybrid coating materials on plexiglass surfaces according to DIN 53151.

In order to determine the coating performance of the UA resin and coating materials, each formulation was applied onto plexiglass panels using an applicator, and then cured in a bench-type UV processor (EMA Group, Turkey), with 120 w cm^{-1} medium pressure mercury UV lamps.

The contact angles (θ) were determined via a sessile drop test method. For each sample, four measurements were made and the average was taken.

The acid resistance of the coating materials were tested by using 10% aqueous solutions of HCl, CH_3COOH, H_2SO_4, and NaOH. Weighed samples were kept in acid solutions for 1 day and then they were weighed to determine the weight loss. The solvent resistance of the prepared samples in various solvents, such as chloroform, xylene, and methanol, were also examined by the same method.

To observe the phase structure of the coating materials, they were examined by a SUPRA 35 VP,

LEO model scanning electron microscope (SEM). The samples were broken under liquid nitrogen and coated with platinum before the analysis.

Results and discussion

Structures characterization of UA resin

The UA resin used to prepare the UV-curable nanohybrid coating materials was synthesized in three steps. Firstly, a diol compound, which is an unsaturated ester, was prepared from 1,2-epoxy cyclohexane and itaconic acid. Then, –NCO-terminated urethane was synthesized by using the diol compound and IPDI. Finally, UV-curable UA resin was prepared from –NCO-terminated urethane and HEMA. Figure 3 shows the FTIR spectra of the –NCO-terminated urethane and UA resin. In the spectrum of the –NCO-terminated urethane, there is a characteristic –NH band at 3362 cm^{-1} and an asymmetric –NCO band at 2257 cm^{-1}. In addition, an aliphatic C–H band at 2935 $cm^{-1}$was seen, with C=O stretching bands of amide at 1695 cm^{-1} and peaks at 1523 cm^{-1} which correspond to amide II. As can be seen in the spectrum of the UA resin, while the peak of –NCO has disappeared, a –NH peak at 3385 cm^{-1} was seen which is characteristic for urethanes, as well as aliphatic C–H at 2935 cm^{-1}, –C=C bands at 1637 cm^{-1} corresponding to acrylates, and C=O stretching bands of amides at 1687 cm^{-1}. These FTIR spectra are consistent with the structure of UA resin.

The structure of UA resin was further characterized by ^{1}H-NMR. Figure 4 displays the ^{1}H NMR spectrum of UA resin in CD_3COCD_3. There are signals at 2.05 ppm for CD_3COCD_3, at 6.66 ppm for (urethane-NH, cyclohexane-OCO-NH-isophoron) protons, at 6.28–6.26 ppm for (urethane-NH, –CH_2–NH–OCO–) protons, at 6.11–6.09 ppm for (acrylate,–OCO–CH_2=C) protons, at 5.63–5.60 ppm for (itaconic acid, C=CH_2) protons, at 4.22-4.17 ppm for (cyclohexane-CH–OCO– and –NHCO-CH_2CH_2-OCO-) protons, at 3.80–3.74 ppm for (–O–CONH–CH-isophoron) protons, at 3.80–3.74 ppm for (-O-CONH-CH-isophoron) protons, at 2.10 ppm for (itaconic acid, OCO– CH_2 –C=C–) protons, at 1.97 ppm for (acriylic, -CH_3) protons, at 1.92–1.90 ppm for (corresponding to cyclohexane –CH_2–CH_2–) protons, at 1.62-1.30 ppm for (corresponding to isophoron –CH_2-CH_2-) protons, and at 0.94-0.90 ppm for (corresponding to isophoron –CH_3, –$C(CH_3)_{2-}$) protons which have proved the structure of the UA resin.

Double bonds conversion of UA resin and nanohybrid materials

Real-time FTIR analyses were performed to examine the double bond conversion percentage (C%). Conversion plots of the C=C bands (at 1637 cm^{-1}) of the UA and nanohybrid materials are shown in Fig. 5. The resin was put on the KBr pellets and subjected to UV light for 3 min to follow the double bond conversion peaks between the first and last seconds by using the FTIR spectra in the range of 400–4000 cm^{-1}.

Conversions of carbon–carbon double bonds were found in the range of 87.77–95.40% in all the nanohybrid formulations. On the other hand, the conversion of carbon–carbon double bonds in the urethane acrylate resin without POSSV is 87.77%. This value

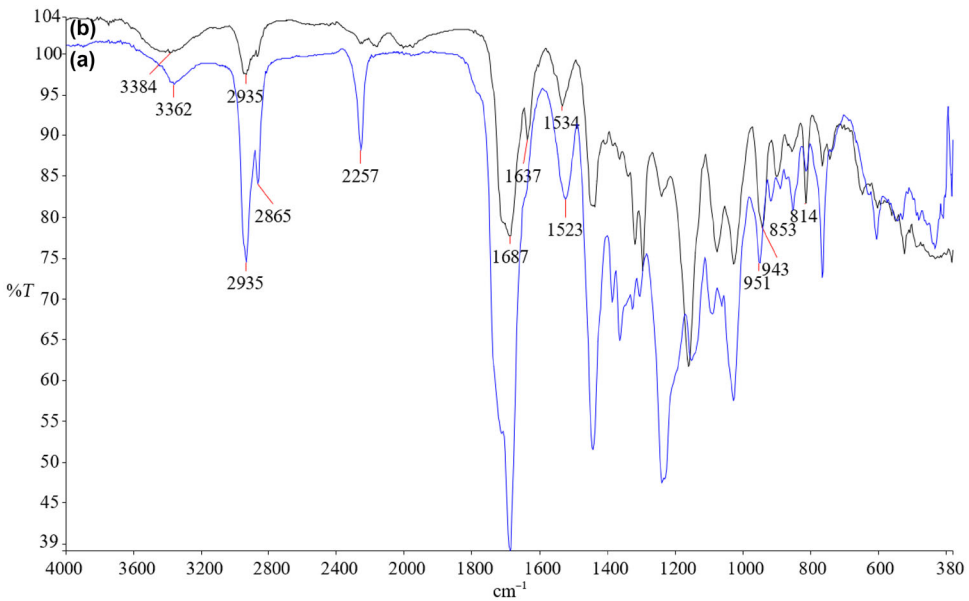

Fig. 3: FTIR spectra of (a) –NCO-terminated polyurethane and (b) UA resin

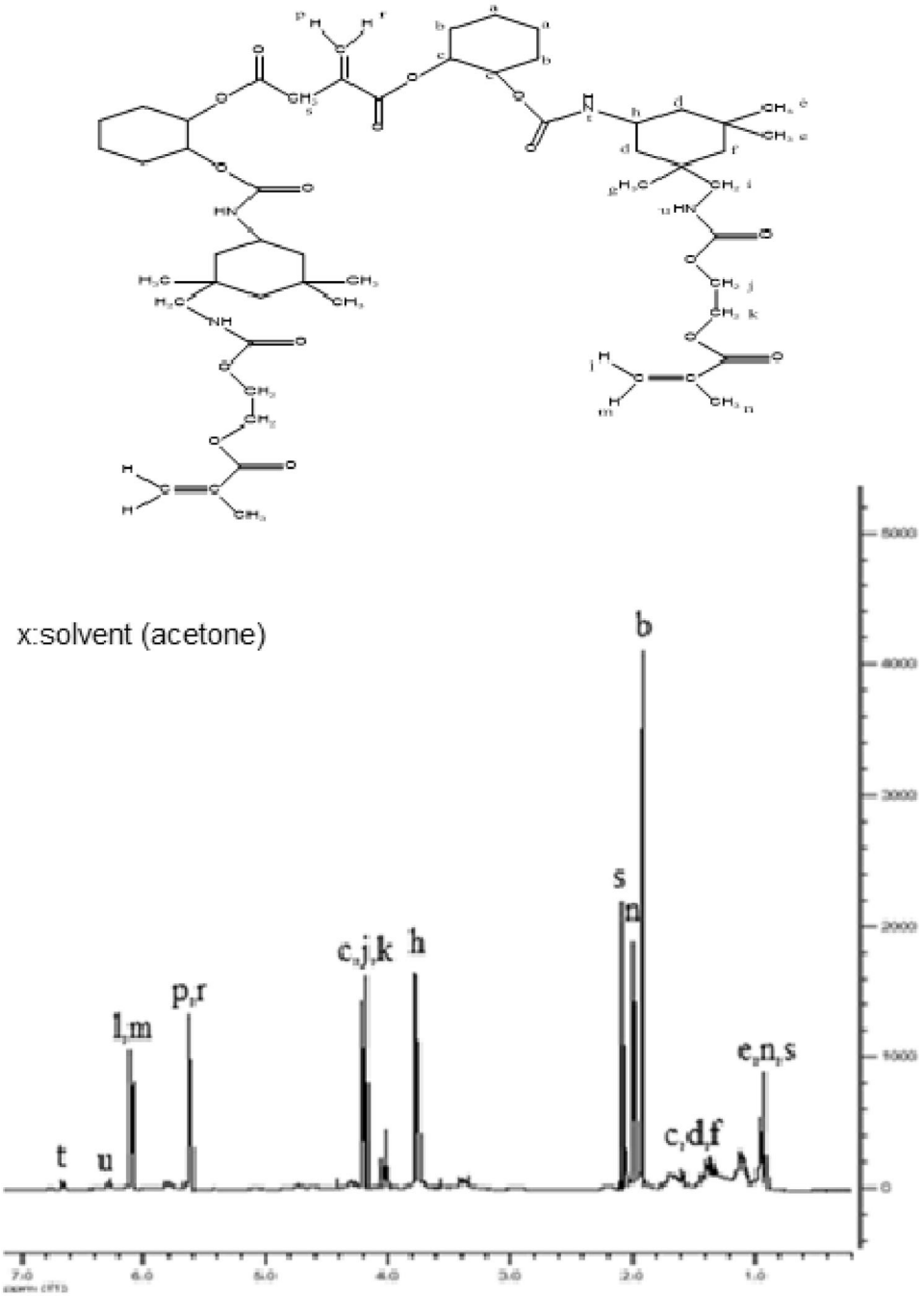

Fig. 4: ^{1}H NMR spectrum of UA resin

increases with the addition of POSSV to the urethane acrylate formulations. This situation might be explained by the increasing carbon–carbon double bond ratios in the UV-curable nanohybrid formulations. In addition, double bond conversions among the nanohybrids containing POSSV increased slightly, as seen in Fig. 5. As a result, compounds that contain vinyl, thiol, and acrylate functional groups can react successfully via the thiol–ene free radical mechanism.

XRD analysis of UA resin and nanohybrid materials

XRD measurements were performed on the UA resin and nanohybrid materials between $2Q$ = 2–40 at 45 kV and 40 mA with a CuK_a radiation (n = 1.54 Å) brand diffractometer, and the results are shown in Fig. 6, from which it can be seen that the most intense peak is at $2Q = 8.22°$ on the XRD graph of POSSV. Apart

from this, it is possible to see less intense peaks in other degrees that reveal the crystallinity of the POSSV. On the other hand, it is not possible to see as many peaks as in the POSSV in the XRD graph of the UA resin and nanohybrid materials. This is due to the amorphous structure resulting from the intense crosslinks formed in the UV curing process. However, when the XRD graph of the UA-POSSV:3 and UA-POSSV:5 samples are examined, there are vague peaks at $2Q = 8.22°$. These peaks are due to POSSV in the structure of the materials. These peaks are rather indistinct in other samples due to intense crosslinking.

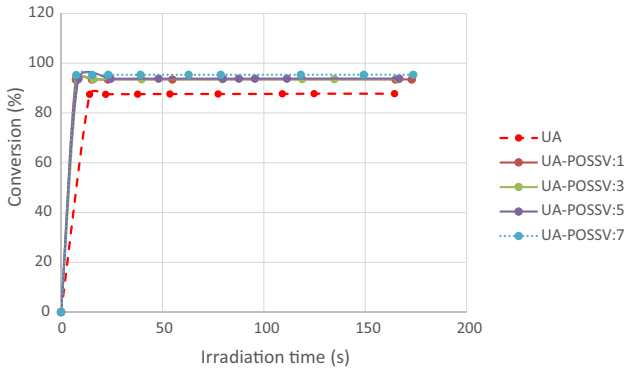

Fig. 5: Conversion percentage (C%) of double bonds (C=C at 1637 cm^{-1}) for the nanohybrids

Thermal properties of UA resin and nanohybrid materials

The thermal properties of the samples were tested using thermogravimetric analysis (TGA). TGA thermograms and the collected data are depicted in Fig. 7 and Table 2, respectively. All the coating films underwent a weight loss of about 5% in the range of 208–223°C. This condition might be derived from residual solvent, unreacted organic compounds such as a photoinitiator, and reactive diluent. As seen in Fig. 7, there are two main weight losses observed in the TGA thermograms. These temperatures correspond to the weight loss of all the coating materials which were not

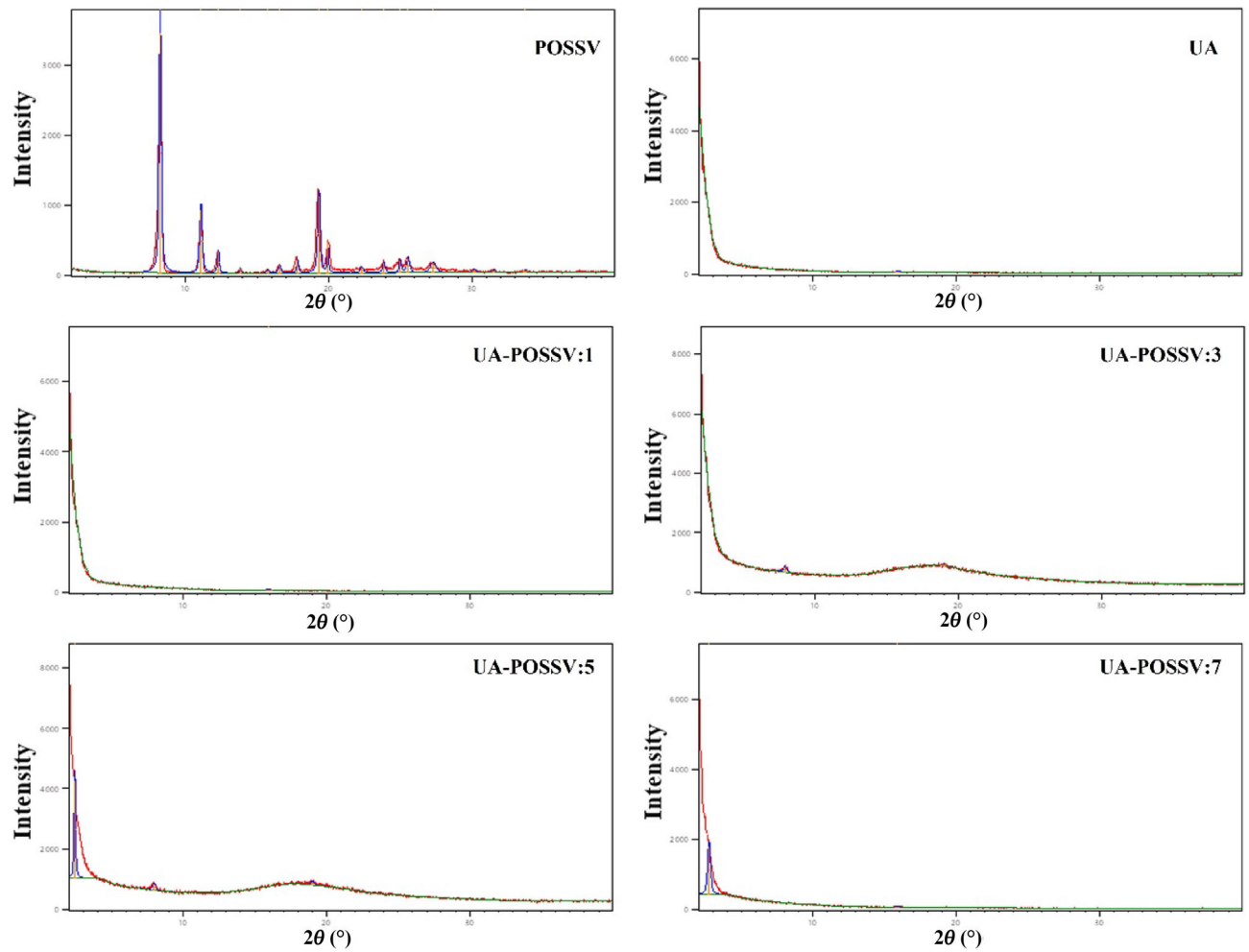

Fig. 6: XRD graphics of UA resin and nanohybrid materials

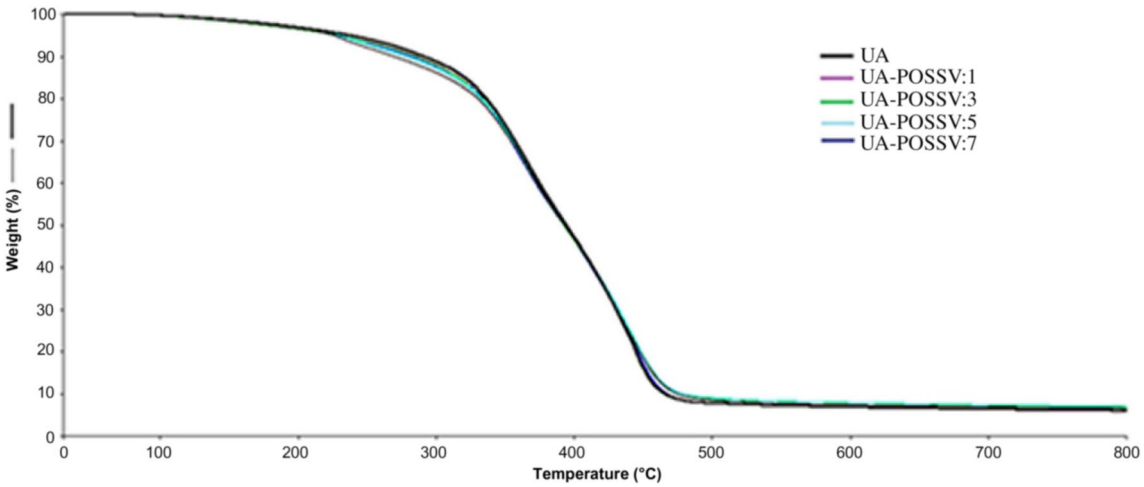

Fig. 7: Thermograms of UA resin and nanohybrid materials

Table 2: Thermal properties of UA resin and nanohybrid materials

Sample	5% weight loss (°C)	First weight loss (°C)	Last weight loss (°C)	Char (%)	LOI (%)	E′ at 30°C (MPa)	E′ at 40°C (MPa)	E′ at 50°C (MPa)
UA	223	322	388	5.36	22	4875	2173	829
UA-1136	POSSV:1	216	328	409	6,01	23	4772	2486
UA-596	POSSV:3	224	323	398	6,70	23	2026	1219
UA-273	POSSV:5	221	322	408	6,44	24	2094	756
UA-557	POSSV:7	208	327	391	7,00	24	3305	1376

shifted meaningfully to higher values when POSSV was added into the UV-curable formulation because of the breaking of the urethane bonds and decomposition of the polymer backbone. As revealed in Table 2, the amount of char ruins increased while the POSSV content increased in the coating formulations in consequence of the increase of silica and the SiO_2 yield produced by the thermal degradation of the POSSV. However, the decomposition temperatures of the coating materials were not changed meaningfully to higher values in the hybrid systems. These situations might have emerged from the steric inhibiton of the POSS nanocages, which probably limited the moving of the polymer chains during the thermal degradation leading to a small increase in the thermal stability.

LOI values of the all samples are given in Table 2 and were between 22 and 24. It can be observed that, when the contents of the POSSV was increased in the formulations, the values of LOI changed slightly.

The curves evaluated from the DMA analysis performed to determine the thermomechanical behavior of the samples are presented in Fig. 8. The storage modules (E′) at 30, 40, and 50 are also listed in Table 2. While the sample prepared with 1% POSSV at 30°C has a lower storage modulus than UA, it appears to have a larger storage modulus at high temperature. However, all the samples (except the 1% doped one) have a lower storage modulus than UA at all temper-

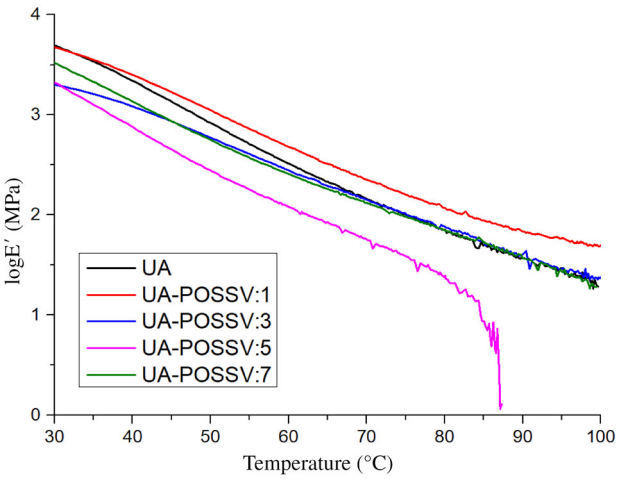

Fig. 8: DMA curves of UA resin and nanohybrid materials

atures. The change in storage module values is not regularly (strictly or directly) dependent on the amount of POSSV. One of the most striking results is that the storage modulus of the UA sample at 50°C is 829 MPa, while that of the UA-POSSV:5 sample is 273 MPa, which is about 67% lower. These results show that the addition of POSSV complexly affects the formation of crosslinks formed during the UV curing process and causes a more flexible structure.

Optical properties of UA resin and nanohybrid materials

The optical properties of the nanohybrid materials were tested using a UV-Vis spectrophotometer. The UV-Vis spectra of all the samples are shown in Fig. 9 and their % transmittance at different wavelengths are given in Table 3. POSSV addition to the UA resin at various ratios decreases the permeability of the materials in the visible region due to the increasing crosslink density. These results are in agreement with the polymeric film images shown in Fig. 2.

Physical characterization of UA resin and nanohybrid materials

The crosslink density of the samples was measured using the Soxhlet extraction method. Weighed film samples of various formulations were extracted with acetone. The insoluble part of the samples was removed from the solution and dried in a vacuum oven at 45ºC. The gel content of the samples was calculated gravimetrically using weights of the samples before and after extraction. As presented in Table 4, the gel content of the nanohybrid materials is in the range of 93–99%. These results in the UV-curable films can be attributed to a high rate of crosslinking and curing.

Nanohybrid materials were subjected to a swelling test in distilled water to measure their water resistance. The swelling ratios shown in Table 4 were found to be very low due to their hydrophobicity which refers to good water resistance. UA resin itself already has good water resistance and the addition of POSSV does not meaningfully affect the swelling properties of the resin.

Cross-cut adhesion tests between the coating materials and the plexiglass substrates were performed according to the DIN 53151 standard. Adhesion is classified on a scale from 0 to 5. Classification limiting values indicate excellent adhesion and poor adhesion, respectively. As seen in Table 4, all the coating formulations exhibit perfect adhesion properties, classified as 0 on the plexiglass panels. These results can be explained by a mutual

Table 3: Transmittance of UA resin and nanohybrid materials

Sample	500 nm T%	600 nm T%	700 nm T%
UA	98	100	100
UA-POSSV:1	97	99	99
UA-POSSV:3	92	96	98
UA-POSSV:5	90	95	97
UA-POSSV:7	89	94	97

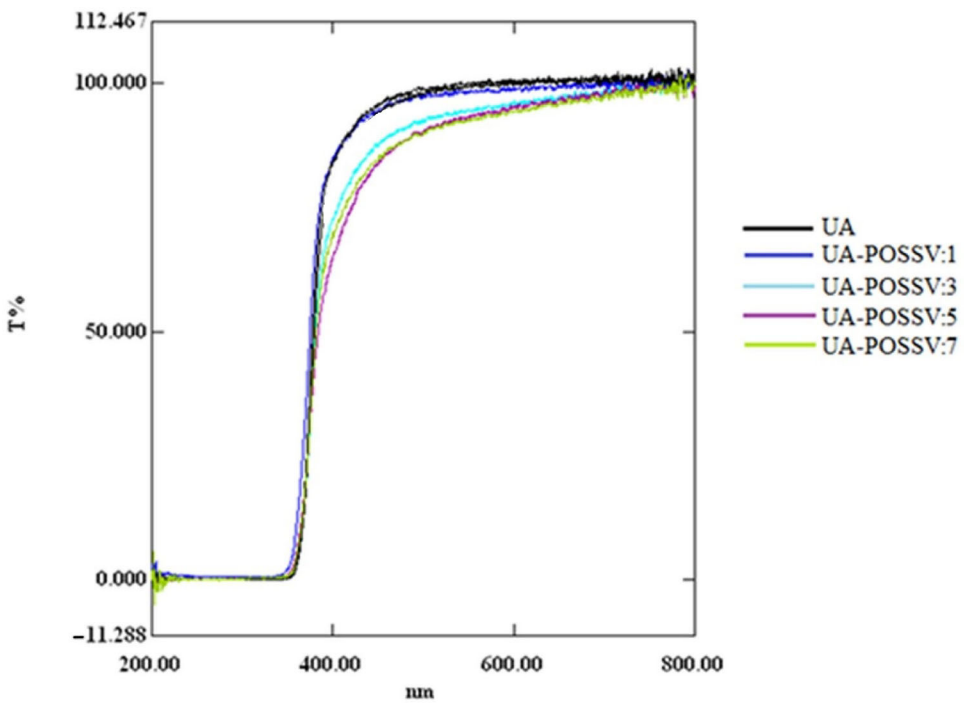

Fig. 9: UV-Vis curves of UA resin and nanohybrid materials

Table 4: Physical characterization of UA resin and nanohybrid materials

Sample	Gel content (wt%)	Swelling ratio (wt%)	Cross-cut adhesion	Damping time (s)	Contact angle (°)
UA	99	0	0	96	76
UA-POSSV:1	97	0.26	0	98	79
UA-POSSV:3	97	0.38	0	101	79
UA-POSSV:5	93	0.88	0	104	79
UA-POSSV:7	95	0.61	0	110	82

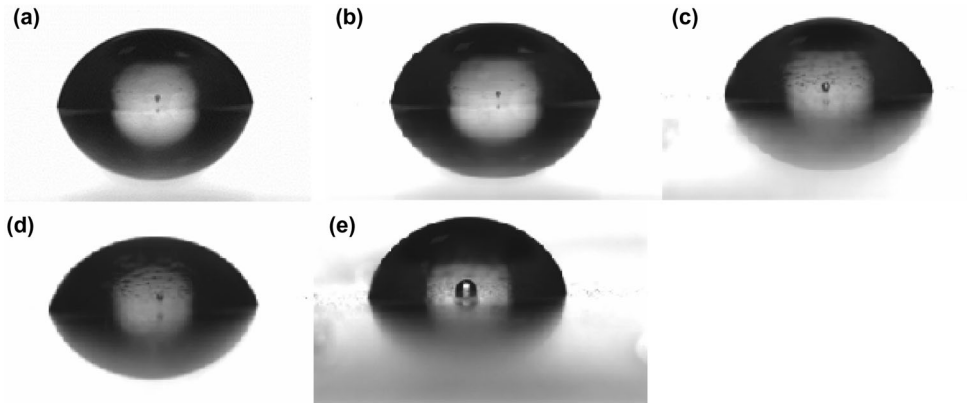

Fig. 10: Contact angle images of coating materials: (a) UA resin, (b) UA-POSSV:1, (c) UA-POSSV:3, (d) UA-POSSV:5, (e) UA-POSSV:7

Table 5: Chemical resistance of UA resin and nanohybrid materials

Sample	HCl (10%)		H_2SO_4 (10%)		CH_3COOH (10%)		NaOH (10%)	
	Appearance	Mass loss wt%	Appearance	Mass loss wt%	Appearance	Mass loss wt%	Appearance	Mass loss wt%
UA	Good	< 1	Good	< 1	Good	< 1	Yellowish	< 20
UA-POSSV:1	Good	< 1	Good	< 1	Good	< 1	Yellowish	< 40
UA-POSSV:3	Good	< 1	Good	< 1	Good	< 2	Yellowish	< 40
UA-POSSV:5	Good	< 1	Good	< 2	Good	< 1	Yellowish	< 20
UA-POSSV:7	Good	< 1	Good	< 1	Good	< 2	Yellowish	< 20

Table 6: Solvent resistance of UA resin and nanohybrid materials

Sample	Xylene		Methanol		Chloroform	
	Appearance	Mass loss (wt%)	Appearance	Mass loss (wt%)	Appearance	Mass loss (wt%)
UA	Good	< 1	Good	< 5	Damaged	< 35
UA-POSSV:1	Good	< 1	Good	< 4	Damaged	< 35
UA-POSSV:3	Good	< 1	Good	< 4	Damaged	< 30
UA-POSSV:5	Good	< 1	Good	< 4	Damaged	< 30
UA-POSSV:7	Good	< 1	Good	< 5	Damaged	< 30

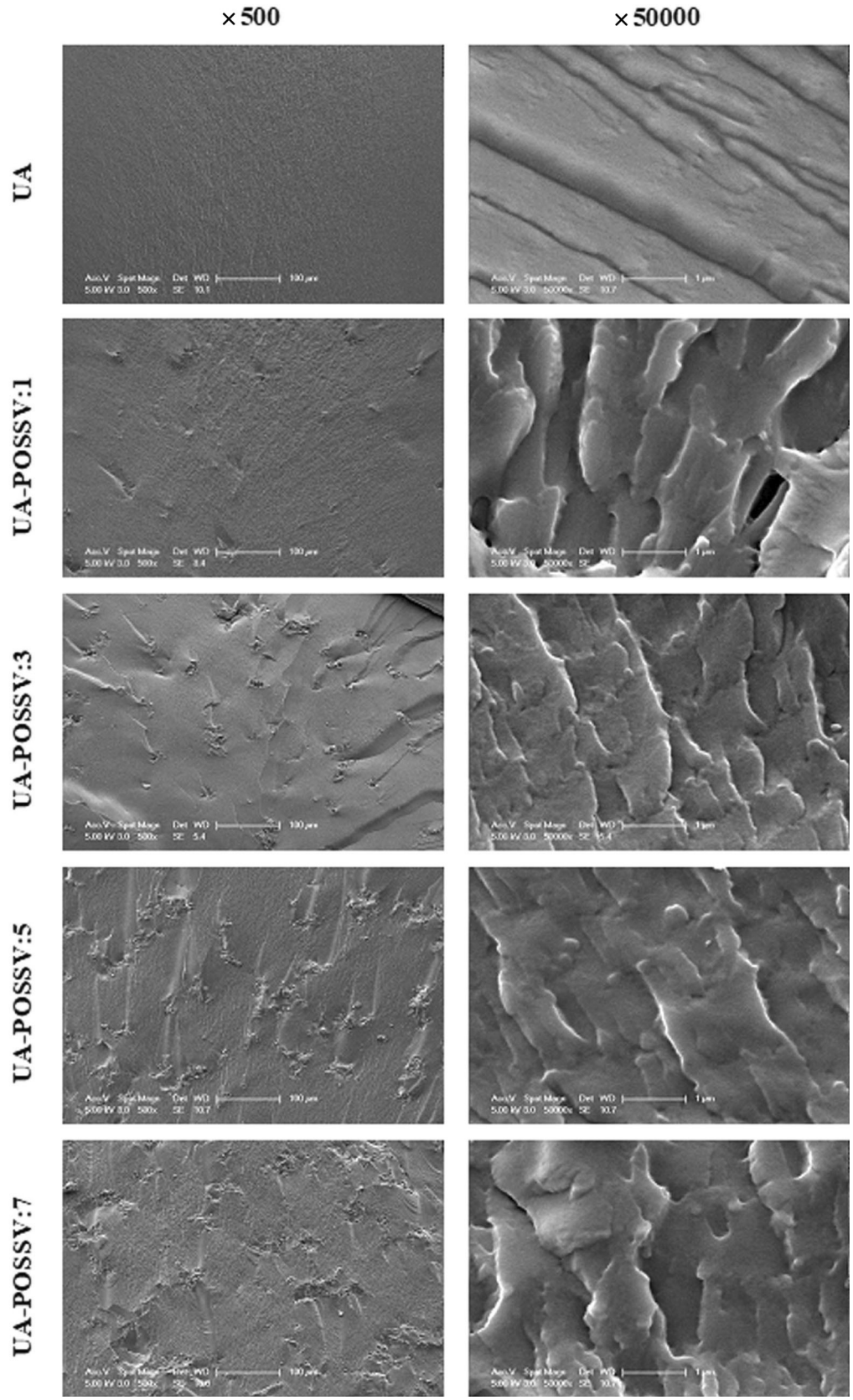

Fig. 11: SEM images of UA resin and nanohybrid materials

good effect between the coating formulations and the plexiglass surfaces. In addition, another reason for the good adhesion can be explained by the treatment of the plexiglass panels with oxygen plasma created by a Ugur Electronic UD-600 Corona Generator under atmospheric pressure (at a power of 1.5 kW at room temperature) before implementing the coating formulation.

A pendulum hardness test was applied to the UA resin and POSSV-modified UA resin-based materials coated on the plexiglass surfaces. The results given in terms of damping time in Table 4 show that the addition of POSSV to the UA resin has increased the hardness of the coating materials.

The hydrophobicity of the coating materials was tested by contact angle measurements in deionized water. The contact angle values of the coating materials are given in Table 4 and their images in Fig. 10. While the contact angle value of UA was 76°, a higher value was observed for the UA-POSSV:7 sample, at 82°. It can be concluded that, by increasing the content of POSSV, more hydrophobic surface was obtained.

Chemical and solvent resistance of UA resin and nanohybrid materials

The results of chemical and solvent resistance tests, based on the mass loss of the nanohybrid films before and after the tests, are presented in Tables 5 and 6, respectively. As can be seen, the mass loss of the films in various chemicals and solvents were found to be less than 1% and their appearance does not change in the chemicals and solvents. It was observed that the hybrid films are slightly damaged in chloroform. However, the physical appearances of the films in the basic medium (NaOH) were yellowish and broken. The results showed that the UA resin and nanohybrid materials were highly resistant to most chemicals and solvents.

Morphologies of UA resin and nanohybrid materials

SEM images of both the UA resin and nanohybrid materials containing POSSV are shown in Fig. 11 at $\times$500 and $\times$50,000 magnifications, from which it can be seen that the inorganic additive (POSSV) has been almost homogeneously dispersed through the polymer matrix when 1% POSSV was added to the UA resin. However, increasing amounts of POSSV in the polymer matrix caused the aglomeration of nanoparticles and also increased the heterogeneity.

Conclusions

We have investigated the effect of the POSSV compound as an inorganic additive on the thermal and physical properties of UA resin-based nanohybrid coating materials. The FTIR and ^{1}H-NMR spectroscopy results showed that the epoxy-based urethane acrylate resin was successfully synthesized. The double bond conversion results proved that the reactions taking place in the UV curing process were quite high. XRD results showed that the nanohybrid films were composed of amorphous and partially crystalline regions due to the POSSV. The TGA and LOI results revealed that the POSSV additive increased the ash yield and inflammability, and, from the DMA results, especially the sample containing 1% POSSV partially preserved the storage modulus value of it at high temperatures. The light transmittance results showed that the samples were more opaque with the POSSV additive. From the physical test results of the coatings, it can be seen that, thanks to the POSSV additive, harder, more hydrophobic, and partially swelling materials were obtained. It was determined that the POSSV additive did not cause a change in the chemical and solvent resistance of the samples. In addition, it was determined from the SEM results that the POSSV additive was homogeneously distributed through the materials but spatial inhomogeneity was also observed in the micrographs with the increasing ratio of POSSV. Thus, nanohybrid materials obtained from the synthesized UA resin and improved by the addition of POSSV can be used in the coating industry.

Acknowledgments This work was supported by Marmara University, Commission of Scientific Research Project under the project FEN-C-YLP-120917-0541.

References

1. Li, X, Qin, Y, Picraux, ST, Guo, ZX, ''Noncovalent Assembly of Carbon Nanotube-Inorganic Hybrids.'' *J. Mater. Chem.*, **21** 7527–7547 (2011)
2. Zhang, WA, Muller, AHE, ''Architecture, Self-assembly and Properties of Well-Defined Hybrid Polymers Based on Polyhedral Oligomeric Silsequioxane (POSS).'' *Prog. Polym. Sci.*, **38** 1121–1162 (2013)
3. Tanaka, K, Ishiguro, F, Kunita, T, Chujo, Y, ''Transparent Conductive Films Based on Polymer Composites Containing the Mixed-Valence Tetrathiafulvalene Nanofibers.'' *J. Polym. Sci. A*, **47** 6441–6450 (2009)
4. Tanaka, K, Adachi, S, Chujo, Y, ''Structure-Property Relationship of Octa-Substituted POSS in Thermal and Mechanical Reinforcements of Conventional Polymers.'' *J. Polym. Sci. A*, **47** 5690–5697 (2009)
5. Wu, L, Glebe, U, Boker, A, ''Surface-Initiated Controlled Radical Polymerizations from Silica Nanoparticles, Gold Nanocrystals, and Bionanoparticles.'' *Polym. Chem.*, **6** 5143–5184 (2015)
6. Akindoyo, JO, Beg, MDH, Gazali, S, Islam, MR, Jeyaratnama, N, Yuvarajc, AR, ''Polyurethane Types, Synthesis and Applications - A Review.'' *RSC Adv.*, **6** 114453–114482 (2016)

7. Reghunadhan, A, Thomas, S, ''Polyurethanes: Structure, Properties, Synthesis, Characterization, and Applications.'' In: Thomas, S, Datta, J, Haponiuk, J, Reghunadhan, A (eds.) *Polyurethane Polymers: Blends and Interpenetrating Polymer Networks*, pp. 1–16. Elsevier, Amsterdam (2017)
8. Kim, BS, Kim, BK, ''Enhancement of Hydrolytic Stability and Adhesion of Waterborne Polyurethanes.'' *J. Appl. Polym. Sci.*, **97** 1961–1969 (2005)
9. Lu, YS, Larock, RC, ''Soybean Oil-Based, Aqueous Cationic Polyurethane Dispersions: Synthesis and Properties.'' *Prog. Org. Coat.*, **69** 31–37 (2010)
10. Okabe, M, Lies, D, Kanamasa, S, Park, EY, ''Biotechnological Production of Itaconic Acid and Its Biosynthesis in *Aspergillus terreus*.'' *Appl. Microbiol. Biotechnol.*, **84** 597–606 (2009)
11. Brannstrom, S, Malmstrom, E, Johansson, M, ''Biobased UV-Curable Coatings Based on Itaconic Acid.'' *J. Coat. Technol. Res.*, **14** 851–861 (2017)
12. Fonseca, AC, Lopes, IM, Coelho, JFJ, Serra, AC, ''Synthesis of Unsaturated Polyesters Based on Renewable Monomers: Structure/Properties Relationship and Crosslinking with 2-hydroxyethyl Methacrylate.'' *React. Funct. Polym.*, **97** 1–11 (2015)
13. Yang, Z, Wicks, DA, Yuan, J, Pu, H, Liu, Y, ''Newly UV-Curable Polyurethane Coatings Prepared by Multifunctional Thiol- and Ene-Terminated Polyurethane Aqueous Dispersions: Photopolymerization Properties.'' *Polymer*, **51** 1572–1577 (2010)
14. Asif, A, Shi, WF, ''UV Curable Waterborne Polyurethane Acrylate Dispersions Based on Hyperbranched Aliphatic Polyester: Effect of Molecular Structure on Physical and Thermal Properties.'' *Polym. Adv. Technol.*, **15** 669–675 (2004)
15. Jančovičová, V, Mikula, M, Havlínová, B, Jakubíková, Z, ''Influence of UV-Curing Conditions on Polymerization Kinetics and Gloss of Urethane Acrylate Coatings.'' *Prog. Org. Coat.*, **76** 432–438 (2013)
16. Wang, F, Hu, JQ, Tu, WP, ''Study on Microstructure of UV-Curable Polyurethane Acrylate Films.'' *Prog. Org. Coat.*, **62** 245–250 (2008)
17. Hong, JW, Cheon, HK, Kim, SH, Hwang, KH, Kim, HK, ''Synthesis and Characterization of UV Curable Urethane Acrylate Oligomers Containing Ammonium Salts for Anti-Fog Coatings.'' *Prog. Org. Coat.*, **110** 122–127 (2017)
18. Zhang, Y, Miao, H, Shi, WF, ''Photopolymerization Behavior and Properties of Highly Branched Polyester Acrylate Containing Thioether Linkage Used for UV Curing Coatings.'' *Prog. Org. Coat.*, **71** 48–55 (2011)
19. Lee, HT, Lin, LH, ''Waterborne Polyurethane/Clay Nanocomposites: Novel Effects of the Clay and Its Interlayer Ions on the Morphology and Physical and Electrical Properties.'' *Macromolecules*, **39** 6133–6141 (2006)
20. Nanda, AK, Wicks, DA, Madbouly, SA, Otaigbe, JU, ''Nanostructured Polyurethane/POSS Hybrid Aqueous Dispersions Prepared by Homogeneous Solution Polymerization.'' *Macromolecules*, **39** 7037–7043 (2006)
21. Zhang, S, Chen, Z, Xu, Z, Gang, S, Bai, H, Liu, X, ''Hydrophobic, Transparent Waterborne UV-Curable Polyurethane Nanocomposites Based on Polycarbonate and PCL-PDMS-PCL Reinforced with Colloidal Silica.'' *J. Coat. Technol. Res.*, **13** 1021–1033 (2016)
22. Lin, HC, Kuo, SW, Huang, CF, Chang, FC, ''Thermal and Surface Properties of Phenolic Nanocomposites Containing Octaphenol Polyhedral Oligomeric Silsesquioxane.'' *Macromol. Rapid Commun.*, **27** 537–541 (2006)
23. Wang, Y, Liu, FG, Xue, XX, ''Synthesis and Characterization of UV-Cured Epoxy Acrylate/POSS Nanocomposites.'' *Prog. Org. Coat.*, **76** 863–869 (2013)